

Probing the Role of (Nd, Ni) Co-doping on Structural and Optical Properties of Nanocrystalline BiFeO₃

Mehroosh Fatema, Anand Somvanshi, Samiya Manzoor, and Shahid Husain^{a)}

Department of Physics, Aligarh Muslim University, Aligarh (INDIA), 202002

^{a)}Corresponding author email: s.husaincmp@gmail.com

Abstract: The pure and (Nd, Ni) co-doped BFO (Bi_{0.9}Nd_{0.1}Fe_{0.9}Ni_{0.1}O₃) nanoparticles have been synthesized using the sol-gel combustion method. The phase purity and crystal structure of the samples are confirmed by the x-ray diffraction pattern. Rietveld refinement analysis is performed to calculate the lattice parameters, bond lengths, and bond angles. The crystal structure of the samples is found to be rhombohedral distorted perovskite structure with space group R3c. The crystallite size is calculated using both Scherrer's relation and Williamson Hall approach and is found to increase with doping. FTIR studies reveal absorptions peaks at 547 cm⁻¹ and 429 cm⁻¹ respectively. These are the characteristic peaks of the FeO₆ octahedra and hence confirm the formation of the BFO phase. The reflectance spectra show a peak at 305 nm in UV region and is transparent to the material in the visible region. The optical band gap has been estimated by using the Tauc's relation and is found to be 2.92 eV for pure and 2.99 eV for (Nd, Ni) co-doped BFO.

Keywords: Rietveld refinement, Williamson Hall method, FTIR

INTRODUCTION

Multiferroics are materials that exhibit coupled electric and magnetic order, leading to the simultaneous existence of ferroelectricity and ferromagnetism [1]. BiFeO₃ (BFO) is a good example of multiferroics as it manifests coexistence of ferroelectricity and antiferromagnetism at room temperature [2]. BFO has rhombohedrally-distorted perovskite structure with R3c space group and reveals ferroelectric (FE) and antiferromagnetic (AFM) (G-type) properties below the Curie temperature (T_C) ~ 1103 K and Neel temperature (T_N) ~ 643 K, respectively [3][4]. In addition, due to its small band gap energy, BFO can utilize a broad range of solar wavelengths in photo-induced applications such as photovoltaic effect and photocatalytic activity [5]. Extensive investigations have been carried out in order to tune the optical band gap of BFO material by introducing the co-doping approach. Wang et al. [6] have demonstrated that Nd substitution at the A-site increases the band gap of BFO ceramic. Venga et al. [7] have reported on the effect of Ni doping at the B-site of Nd-doped BFO. But these type of studies are scarce in the literature. Therefore we undertook the synthesis of BFO and (Nd, Ni) co-doped BFO to study the effect of co-doping on its structural and optical properties.

EXPERIMENTAL

Nanocrystalline samples of pristine BFO and (Nd, Ni) co-doped BFO were synthesized by the sol-gel combustion method (chemical route). The initial precursors, [Bi(NO₃)₃.5H₂O], [Fe(NO₃)₃.9H₂O], [Nd(NO₃)₂.6H₂O] and [Ni(NO₃)₂.6H₂O] were taken in a stoichiometric ratio and a solution was prepared. Citric acid was used as a catalyst to enhance the reaction rate and ethylene glycol was used to promote the formation of gel. In order to ensure the formation of a homogeneous solution without the presence of any precipitates, nitric acid was slowly added to the mixture followed by ammonia to maintain a pH value close to 4. The solution was constantly stirred at 80°C for 5 hours to obtain a xerogel. The xerogel was sintered at 200°C for 4 hours and calcined at 600°C for 2 hours to obtain the final products.

The formation of the samples was confirmed by the x-ray diffraction (XRD) using Shimadzu LabX XRD-6100 advance diffractometer (Cu-K_α radiation, λ= 1.54 Å) in the 2θ angle from 20° to 80° with the step size of 0.02°. The Rietveld refinement of the XRD profile is carried out using the Full Prof software. The FTIR Spectra was recorded within the range 400 cm⁻¹ to 4000cm⁻¹ using Bruker Tensor 37 spectrometer. The band gap energy was

evaluated using the spectra recorded by the UV-Vis Spectrometer (Perkin Elmer, Lambda 950) in the wavelength region 200-800 nm.

RESULTS AND DISCUSSION

XRD patterns of pristine and (Nd, Ni) co-doped BFO samples have been analyzed with the Rietveld refinement method, to determine the structural information of the samples (Fig. 1). In the refinement, pseudo-Voigt function and the twelve-order polynomial were used to define the profileshape and background respectively. The observed diffraction peaks of doped BFO exhibit rhombohedral perovskite structure (R3c), similar to BFO. The impurity present around $2\theta = 29^\circ$ corresponds to $\text{Bi}_4\text{Fe}_4\text{O}_9$ and $\text{Bi}_{24}\text{Fe}_2\text{O}_3$. With doping, the double peaks at (104) and (110), (113) and (006) and (116) and (122), merge, revealing a distortion in the rhombohedral structure [7]. The refined cell parameters have been tabulated in Table 1 and Table 2. Goldschmidt's tolerance factor is the measure of stability and distortion of crystal structures. It can be used to describe perovskite structure as well as to calculate the compatibility of an ion with a crystal structure [8], and is calculated by the formula:

$$\tau = (R_A + R_O) / \sqrt{2} (R_B + R_O) \quad (1)$$

where R_A represents the radius of cation A, R_B represents the radius of cation B and R_O denotes the radius of the anion (usually Oxygen). The tolerance factor (τ) has been calculated as 0.848 and 0.855 for BFO and co-doped sample, respectively. Its value for rhombohedral structure lies between 0.71 to 0.9 and an increase in its value indicates a distortion in the crystal structure of the doped BFO, which confirms the results obtained from the Rietveld analysis.

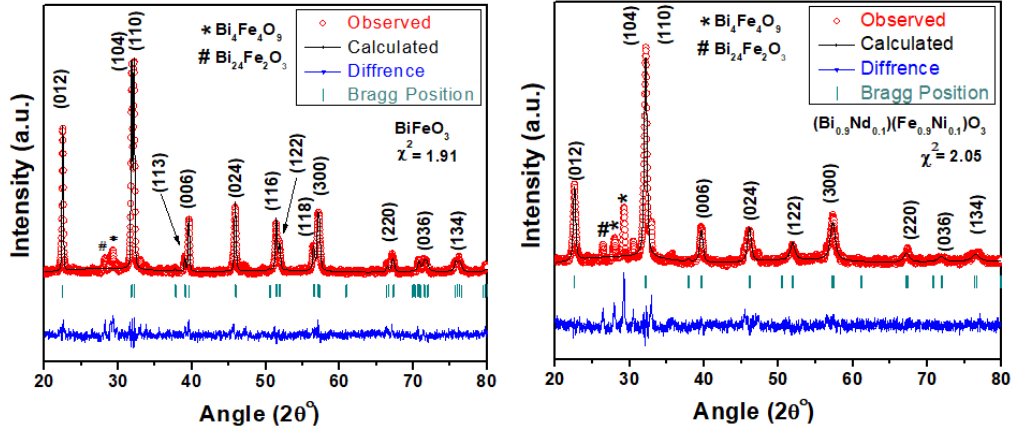


FIGURE 1. XRD patterns of pristine and (Nd, Ni) co-doped BFO with their Rietveld refinement.

TABLE 1. Structural parameters for pristine and co-doped BFO as determined from Rietveld refinement.

Element	Wyckoff Site	x	y	z	$B_{iso}(\text{\AA}^2)$
Bi/Nd	6(a)	0.0000	0.0000	0.05372	0.6
Fe/Ni	6(b)	0.0000	0.0000	0.27525	0.6
O	18(b)	0.45114	0.03038	0.0033	0.6

TABLE 2. Lattice parameters, crystallite size, strain, bond angles and bond length of pristine and (Nd,Ni) co-doped BFO.

Composition	BiFeO_3	$(\text{Bi}_{0.9}\text{Nd}_{0.1})(\text{Fe}_{0.9}\text{Ni}_{0.1})\text{O}_3$
Lattice Parameter (\AA)	a=b=5.5693	a=b=5.5626
	c=13.8457	c=13.7416
Unit Cell Volume (\AA^3)	371.9176	368.2337
χ^2	1.91	2.05
Lattice Strain ($\times 10^{-3}$)	0.92	3.39
Crystallite Size, D (nm)	33	40
Ionic Radii (\AA)		
	Bi^{3+} or/and Nd^{3+}	1.03
	Fe^{3+} or/and Ni^{3+}	0.645
	O^{2-}	1.28
Tolerance factor (τ)	0.848	0.855
Bond Angle ($^\circ$)	Fe-O-Fe	155.232
Bond Length (\AA)	Fe-O	1.8895

The average crystallite size 'D' is calculated using the Scherrer's equation given by:

$$D = k\lambda / \beta \cos\theta \quad (2)$$

where k is a dimensionless shape factor, with a value of about 0.9, that differs with the shape of the crystallite, β is the line broadening at half the maximum intensity (FWHM) and θ is the Bragg angle [9]. The width of the Bragg peak incorporates instrument and sample dependent effects. The instrument corrected broadening β_D corresponds to the diffraction peak of BFO, and is estimated by using the relation:

$$\beta_D^2 = (\beta_{measured}^2 - \beta_{instrumental}^2) \quad (3)$$

On substituting the value of β_D from equation (3) to equation (2), we get the Scherrer's equation as

$$D = k\lambda / \beta_D \cos\theta \quad (4)$$

The average crystallite size calculated from Scherrer's formula was found to be 17 nm for BFO and 20 nm for co-doped BFO respectively.

The Williamson-Hall analysis includes the strain-induced broadening ($\beta_s = 4\epsilon \tan\theta$) arising from crystal imperfections and can be estimated by replacing β with $\beta = \beta_s + \beta_D$, thus giving the following relation:

$$\beta = (k\lambda / D \cos\theta) + 4\epsilon \tan\theta \quad (5)$$

First term ($k\lambda / D \cos\theta$) represents the size broadening and the second term, $4\epsilon \tan\theta$, represents the microstrain broadening [9].

Rearranging (5) gives:

$$\beta \cos\theta = (k\lambda / D) + 4\epsilon \sin\theta \quad (6)$$

The lattice strain has been determined from the slope of the plot between $\beta \cos\theta$ and $4\sin\theta$ (Fig.2) and its value for BFO and co-doped BFO is found to be 0.92×10^{-3} and 3.39×10^{-3} respectively. The value of crystallite size D as calculated from the Williamson Hall plot is slightly higher (33 nm for BFO and 40 nm for co-doped BFO) as compared to the values calculated using the Scherrer's equation, as it includes the effect of strain too.

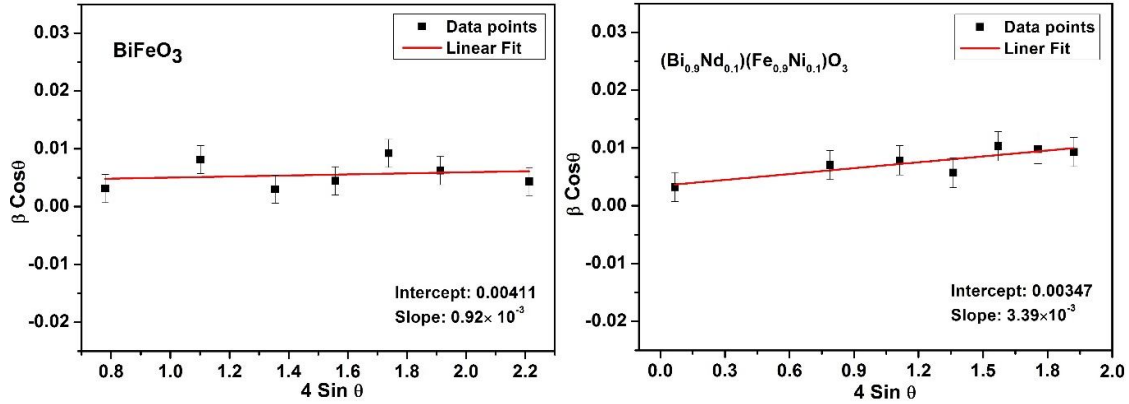


FIGURE 2. Williamson Hall plots for pristine and (Nd, Ni)co-doped BFO

FTIR spectra of BFO and co-doped BFO samples are recorded (Fig.3) to grasp the idea of the different vibrational modes and functional groups present. The fundamental absorption peaks observed at 547 cm^{-1} and 429 cm^{-1} are attributed to the Fe-O stretching vibration mode along the Fe-O axis and the bending vibration mode of the Fe-O bond in the FeO_6 octahedral unit [10]. These bands are the characteristic band of the FeO_6 octahedra and confirm the formation of the BFO phase. The broadbands in the range of $3000\text{-}3600 \text{ cm}^{-1}$ are attributed to the anti-symmetric and symmetric stretching of H_2O and OH groups, while a band at 1625 cm^{-1} corresponds to the bending vibrations of H_2O . The band around 1390 cm^{-1} is the result of the presence of trapped nitrates. The presence of carbonate groups is signified by the bands at $1300\text{-}1500 \text{ cm}^{-1}$, as well as at $1030\text{-}1200 \text{ cm}^{-1}$ and 850 cm^{-1} .

The optical band gap of pristine and (Nd, Ni) co-doped BFO is calculated by the UV-Visible diffuse reflectance spectra, using the Tauc's relation

$$(\alpha h\nu) = A(h\nu - E_g)^n \quad (7)$$

where α is the absorption coefficient, which is proportional to the Kubelka-Munk Function $F(R)$, A is an energy independent constant of the absorption frequency, h is Planck's constant, E_g stands for the optical band gap energy, ν is the frequency of the incident photon and n depends on nature of the transitions involved in the optical absorption [11]. Here, $n=1/2$ refers to direct allowed transitions and $n=2$ for indirect allowed transitions.

The Fig. 4 shows the Tauc's plot of the parent and doped samples. The intercept obtained on the abscissa by extrapolating the linear portion of the $[F(R)h\nu]^2$ versus incident photon energy (hv) plot, gives the optical band

gap[12][13]. The optical band gap energy is found to be 2.92 eV for pure BFO and 2.99 eV for (Nd, Ni) co-doped BFO respectively. The variation in the band gap may be attributed to changes in lattice parameters or FeO_6 octahedra.

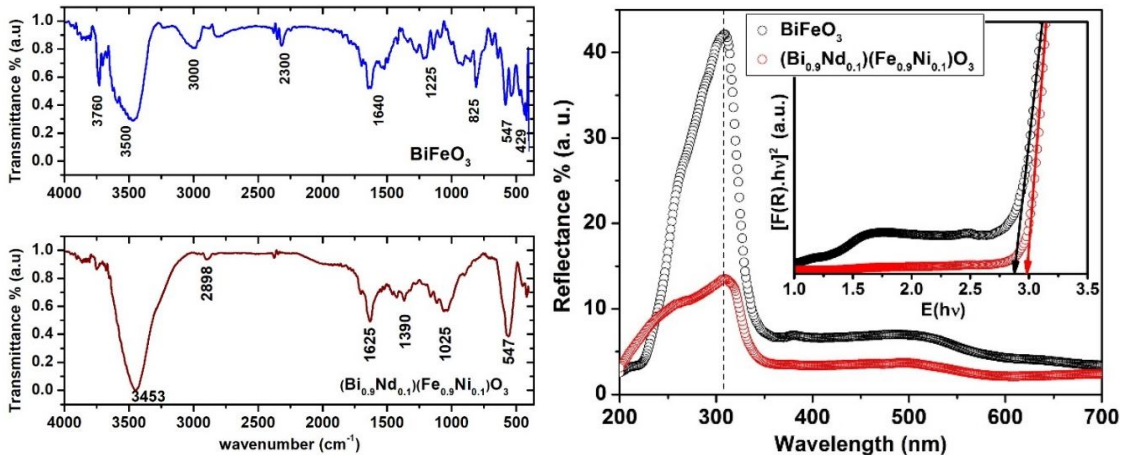


FIGURE 3. FTIR spectra of pure and (Nd, Ni) co-doped BFO. **FIGURE 4.** Reflectance spectra and $[F(R)hv]^2$ versus $E(hv)$ plot of pure and (Nd, Ni) co-doped BFO.

CONCLUSIONS

BFO and (Nd, Ni) co-doped BFO samples have been synthesized using the sol-gel method. XRD patterns and Rietveld refinement reveal that BFO crystallizes in a rhombohedral perovskite structure with the space group $R3c$. Crystallite sizes as calculated from the Scherrer equations are found to increase from 33 nm to 40 nm, with the addition of the dopant. This increase may be due to the doping of bigger ionic radius of Nd^{3+} (1.109\AA) as compared to Bi^{3+} (1.03\AA) ions. The spectra of the synthesized samples obtained by FTIR spectroscopy exhibit fundamental absorptions bands at 429 cm^{-1} and 547 cm^{-1} , confirming the presence of Fe-O stretching (ν_1) and bending (ν_2) vibrational modes. The reflectance spectra show a peak at 305 nm in UV region and are transparent to the material in the visible region. The optical band gap has been estimated by using the Tauc's relation and is found to be 2.92 eV for BFO and 2.99 eV for (Nd, Ni) co-doped BFO.

ACKNOWLEDGMENT

Mehroosh Fatema thanks DST, Government of India for providing financial support under the INSPIRE Fellowship Program (DST/INSPIRE Fellowship/2017/IF170728). Anand Somvanshi thanks UGC-DAE Consortium for Scientific Research (CSR), Mumbai for providing financial support under the project CRS-M-271. The authors would also like to acknowledge Dr. Mohd Jane Alam, Spectroscopy Lab, Department of Physics, A.M.U., Aligarh for the FTIR measurements.

REFERENCES

1. Spaldin, Nicola, Fiebig, and Manfred, *Science*. **309**, 391–2(2005)
2. Kubel, Frank, Schmid, and Hans, *Acta Crystallographica*. **B46**, 698–702(1990)
3. Catalan, Gustau, Scott, and James F, *Advanced Materials*. **21 (24)**, 2463–2485(2009)
4. Kiselev, S. V. Ozerov, R. P. Zhdanov et. al., *Soviet Physics Doklady*. **7(8)**, 742–744(1963)
5. McDonnel, Kevin, Niall et. al, *Chemical Physics Letters*. **572**, 78-84 (2013)
6. Dawei Wang, Meili Wang, Fengbin Liu et. al, *Ceramics International*. **41(7)**, 8768-8772 (2015)
7. Pradeep Reddy Vanga, RV Mangalaraja, M. Ashoka, *Material Research Bulletin*. **72**, 299-305(2015)
8. Xianchun, Liu, Ronghi, Hong et. al. *J Mater Sci: Materials in Electronics*. **20**, 232-327(2009)
9. A. Khorsand Zak, WH. Abd. Majid et. al, *Solid State Sciences*. **13**, 251-256(2011)
10. Heng Wu, Piaojie Xue, Yao Lu, and Xinhua Zhu, *Journal of Alloys and Compounds*. **731**, 471-477(2018).
11. K. Sarkar, Soumya Mukherjee, and M.K. Mitra, *J. Inst. Eng. India*. **95(2)**, 135-143(2014)
12. S. Manzoor and S. Husain, *Mater. Res Express*. **5**, 055009 1-12 (2018)
13. A. Somvanshi, S. Manzoor, and S. Husain, *AIP Conf. Proc.* **1953**, 030243 1-4 (2018)